World Journal of Gastroenterology

Submit a Manuscript: http://www.f6publishing.com

World J Gastroenterol 2018 February 28; 24(8): 929-940

DOI: 10.3748/wjg.v24.i8.929

ISSN 1007-9327 (print) ISSN 2219-2840 (online)

ORIGINAL ARTICLE

Retrospective Study

Intravoxel incoherent motion diffusion-weighted magnetic resonance imaging for predicting histological grade of hepatocellular carcinoma: Comparison with conventional diffusion-weighted imaging

Shao-Cheng Zhu, Yue-Hua Liu, Yi Wei, Lin-Lin Li, She-Wei Dou, Ting-Yi Sun, Da-Peng Shi

Shao-Cheng Zhu, Yue-Hua Liu, Lin-Lin Li, She-Wei Dou, Da-Peng Shi, Department of Radiology, Henan Provincial People's Hospital, Zhengzhou 450003, Henan Province, China

Yue-Hua Liu, Medical College of Henan University, Kaifeng 475000, Henan Province, China

Yi Wei, Department of Radiology, West China Hospital, Sichuan University, Chengdu 610000, Sichuan Province, China

Ting-Yi Sun, Department of Pathology, Henan Provincial People's Hospital, Zhengzhou 450003, Henan Province, China

ORCID number: Shao-Cheng Zhu (0000-0003-4553-1940); Yue-Hua Liu (0000-0002-8971-5947); Yi Wei (0000-0003-3993-9747); Lin-Lin Li (0000-0003-2245-2983); She-Wei Dou (0000-0002-8434-7751); Ting-Yi Sun (0000-0003-4616-744X); Da-Peng Shi (0000-0002-2561-7475).

Author contributions: All the authors were involved in performing the research; Zhu SC, Liu YH, Wei Y, Li LL and Shi DP participated in the study design; Zhu SC, Liu YH, Wei Y, Li LL and Dou SW conducted the experiments; Zhu SC and Liu YH participated in the MR image analyses; Sun TY analyzed the histopathological images; Zhu SC, Liu YH and Wei Y analyzed the data; Zhu SC and Liu YH prepared the first draft of the manuscript; Zhu SC, Liu YH and Wei Y revised the manuscript. Shao-Cheng Zhu and Yue-Hua Liu contributed equally to this article.

Institutional review board statement: This study was reviewed and approved by the Ethics Committee of the Henan Provincial People's Hospital.

Informed consent statement: The patients were not required to give informed consent for the study because the analysis used anonymous clinical data that were obtained after each patient agreed to the MRI examination by written consent.

Conflict-of-interest statement: All the authors declare no conflicts of interest related to this article.

Open-Access: This article is an open-access article which was selected by an in-house editor and fully peer-reviewed by external reviewers. It is distributed in accordance with the Creative Commons Attribution Non Commercial (CC BY-NC 4.0) license, which permits others to distribute, remix, adapt, build upon this work non-commercially, and license their derivative works on different terms, provided the original work is properly cited and the use is non-commercial. See: http://creativecommons.org/licenses/by-nc/4.0/

Manuscript source: Unsolicited manuscript

Correspondence to: Shao-Cheng Zhu, MD, PhD, Chief Doctor, Professor, Department of Radiology, Henan Provincial People's Hospital, No. 7, Weiwu Road, Zhengzhou 450003, Henan Province, China. 104753150948@vip.henu.edu.cn
Telephone: +86-371-65580790

Received: December 21, 2017
Peer-review started: December 21, 2017
First decision: January 3, 2018
Revised: January 11, 2018
Accepted: January 18, 2018
Article in press: January 18, 2018
Published online: February 28, 2018

Abstract

AIM

To compare intravoxel incoherent motion (IVIM)-derived parameters with conventional diffusion-weighted imaging (DWI) parameters in predicting the histological grade of hepatocellular carcinoma (HCC) and to evaluate the correlation between the parameters and the histological grades.

METHODS

A retrospective study was performed. Sixty-two patients with surgically confirmed HCCs underwent diffusion-weighted magnetic resonance imaging with twelve *b* values (10-1200 s/mm^2). The apparent diffusion coefficient (ADC), pure diffusion coefficient (D), pseudo-diffusion coefficient (D*), and perfusion fraction (*f*) were calculated by two radiologists. The IVIM and conventional DWI parameters were compared among the different grades by using analysis of variance (ANOVA) and the Kruskal-Wallis test. Receiver operating characteristic (ROC) analysis was performed to evaluate the diagnostic efficiency of distinguishing between low-grade (grade 1, G1) and high-grade (grades 2 and 3, G2 and G3) HCC. The correlation between the parameters and the histological grades was assessed by using the Spearman correlation test. Bland-Altman analysis was used to evaluate the reproducibility of the two radiologists' measurements.

RESULTS

The differences in the ADC and D values among the groups with G1, G2, and G3 histological grades of HCCs were statistically significant ($P < 0.001$). The D* and *f* values had no significant differences among the different histological grades of HCC ($P > 0.05$). The ROC analyses demonstrated that the D and ADC values had better diagnostic performance in differentiating the low-grade HCC from the high-grade HCC, with areas under the curve (AUCs) of 0.909 and 0.843, respectively, measured by radiologist 1 and of 0.911 and 0.852, respectively, measured by radiologist 2. The following significant correlations were obtained between the ADC, D, and D* values and the histological grades: $r = -0.619$ ($P < 0.001$), $r = -0.628$ ($P < 0.001$), and $r = -0.299$ ($P = 0.018$), respectively, as measured by radiologist 1; $r = -0.622$ ($P < 0.001$), $r = -0.633$ ($P < 0.001$), and $r = -0.303$ ($P = 0.017$), respectively, as measured by radiologist 2. The intra-class correlation coefficient (ICC) values between the two observers were 0.996 for ADC, 0.997 for D, 0.996 for D*, and 0.992 for *f* values, which indicated excellent inter-observer agreement in the measurements between the two observers.

CONCLUSION

The IVIM-derived D and ADC values show better diagnostic performance in differentiating high-grade HCC from low-grade HCC, and there is a moderate to good correlation between the ADC and D values and the histological grades.

Key words: Intravoxel incoherent motion; Diffusion-weighted imaging; Hepatocellular carcinoma; Pathological differentiation grade

© The Author(s) 2018. Published by Baishideng Publishing Group Inc. All rights reserved.

Core tip: Intravoxel incoherent motion (IVIM)-based diffusion-weighted imaging (DWI) can yield diffusion and perfusion information simultaneously. The aims of this study were to compare IVIM-derived parameters with conventional DWI parameters for predicting the histological grade of hepatocellular carcinoma (HCC) and to evaluate the correlation between the parameters and the histological grades. Sixty-two patients with surgically confirmed HCC underwent diffusion-weighted magnetic resonance imaging with twelve *b* values. The differences in the ADC and D values among the groups with G1, G2, and G3 histological grades of HCC were statistically significant ($P < 0.001$). The D* and *f* values had no significant differences among the different histological grades of HCC ($P > 0.05$). A significant correlation was obtained between the ADC, D, and D* values and the histological grades ($P < 0.05$). The ROC analyses demonstrated that the D and ADC values had better diagnostic performance in differentiating low-grade HCC from high-grade HCC. These results suggested that the IVIM-DWI parameters might be useful in assessing the differentiation grades of HCC, which might be helpful in predicting the patient prognosis.

Zhu SC, Liu YH, Wei Y, Li LL, Dou SW, Sun TY, Shi DP. Intravoxel incoherent motion diffusion-weighted magnetic resonance imaging for predicting histological grade of hepatocellular carcinoma: Comparison with conventional diffusion-weighted imaging. *World J Gastroenterol* 2018; 24(8): 929-940 Available from: URL: http://www.wjgnet.com/1007-9327/full/v24/i8/929.htm DOI: http://dx.doi.org/10.3748/wjg.v24.i8.929

INTRODUCTION

Hepatocellular carcinoma (HCC) is the most common primary malignant tumor of the liver, accounting for 85% or more of cases[1]. It is the fifth most important cancer worldwide because of its very poor prognosis, with survival rates of 3% to 5% in the United States and developing countries. Therefore, it is the third leading cause of cancer-related death[2-4]. The pathological grade of a hepatocellular carcinoma is heavily associated with the prognosis, and it is one of the independent predictive factors for recurrence and long-term survival after hepatic curative resection in patients with HCC[5,6]. However, it is difficult to define accurate preoperative grade of HCC using routine imaging modalities. The ultrasound (US)-guided biopsy has been used to diagnose HCC, but this approach is limited due to location and complication risk, such as bleeding or needle-tract seeding, which suggests that it should not be performed in routine clinical practice[7]. Computed tomography (CT) is usually used to identify locations and to assess distant metastasis of HCC, and the performance characteristics of CT also allow it to be used for HCC diagnosis or staging. In terms of triphasic dynamic enhanced CT scans and dynamic

contrast-enhanced magnetic resonance imaging (DCE-MRI), the typical imaging feature of an HCC is that the lesion shows arterial hypervascularity and washes out in the early or delayed venous phase, which can be demonstrated for diagnosis[8]. However, both of these imaging techniques failed to provide a prediction of the pathological grade of an HCC.

Diffusion-weighted imaging (DWI) is a noninvasive approach to sensitively evaluate the small-scale motion of water molecules at the microscopic level that allows the diffusion of water to be quantitatively described by the apparent diffusion coefficient (ADC), which represents a mean value of diffusion contributed by the movement of intracellular, extracellular, and vascular water molecules within an image voxel at different *b* values[9,10]. In addition, these motions include the molecular diffusion of water and microcirculation of the blood in the capillary networks (perfusion). Several studies have shown that DWI, along with ADC measurements, is helpful for the detection, characterization, and staging of malignant lesions[11]. However, the ADC value that is derived from DWI is calculated using the mono-exponential model; therefore, it is often higher than expected, which is attributable to the microcirculation of the blood in capillaries[12]. The ADC value ignores the effect of the perfusion fraction in tissue and could be influenced by microcirculation of the blood in capillaries and cannot reflect the true diffusion of water[13]. Thus, it is limited in that the ADC fails to evaluate the water molecular diffusion in tissues precisely. In 1986, some researchers noted the principles of intravoxel incoherent motion (IVIM) and proposed that the relationship between signal attenuation in tissues with increasing *b* values would estimate the quantitative parameters that separately reflect tissue diffusivity and tissue microcapillary perfusion with the IVIM imaging method[14,15]. The IVIM approach uses a bi-exponential function to describe the DWI data and assumes that the measured signal attenuation of the DWI scans consists of a mixture of tissue perfusion and tissue diffusivity effects. Using the IVIM-based analysis, it is possible to obtain additional quantitative parameters that describe water diffusivity, perfusion (pseudodiffusion coefficient), and the perfusion fraction of tissues, which can also be displayed as parametric maps[12].

Recently, IVIM-DWI has been used to investigate the correlation between the parameters involved in the histological grade of HCC[16-18]. However, knowledge of the measurement reproducibility is critical to the level of confidence that can be ascribed to changes in the parameters for disease characterization or response assessment; this technique can also be developed as a potential imaging biomarker[19]. Therefore, it is important to assess the measurement reproducibility of parameters by different observers. The purpose of our study was to compare IVIM-derived parameters with conventional DWI-derived ADC values for determining the histologic grades of HCC and evaluate the correlation between the parameters and the histological grades.

MATERIALS AND METHODS

Patients

The institutional review board of the Henan Provincial People's Hospital approved this study, and written informed consent was obtained from all the patients. This study was conducted in accordance with the Declaration of Helsinki. Between March 2016 and May 2017, 102 consecutive patients suspected of having HCC underwent liver MR imaging. Among these patients, 40 were excluded for the following reasons: (1) the absence of surgery and/or histopathological examination (n = 14); (2) a history of preoperative treatment (radiofrequency ablation or transarterial chemoembolization) before MR imaging (n = 11); (3) liver lesions that were determined not to be HCC by pathological tests (n = 7); (4) low image quality (n = 3); and (5) tumors that were smaller than 1 cm (n = 5). Finally, a total of 62 patients diagnosed with HCC were included for analysis. The patients comprised 50 men and 12 women (mean age, 54.31 ± 9.36 years; range, 30-76 years). Forty-nine patients tested positive for the hepatitis B surface antigen and six for the hepatitis C virus antibody. The remaining seven patients tested negative for both antigens. According to Child-Pugh class, 54 patients had Child-Pugh A5, 6 had Child-Pugh A6, 2 had Child-Pugh B, and nobody had Child-Pugh C. All the tumors were histologically classified according to the major Edmondson-Steiner grade on the final pathologic reports as follows: grade 1 (n = 14), grade 2 (n = 24), grade 3 (n = 24), and grade 4 (n = 0).

MR imaging technique

All the patients were instructed to fast for 6-8 h prior to the MR examination. The studies were carried out by using a 3.0 T MR system (Discovery MR750, GE Healthcare, MI, United States) with an eight-channel phased-array torsion coil (GE Medical System). The routine MR imaging was performed using a fast spin echo (FSE) sequence with respiratory gating. The axial T1 images were obtained using the following parameters: repetition time/echo time (TR/TE), 180/2.1 ms; slice thickness, 7.0 mm with a gap of 1.0 mm; field of view, 38 cm × 34.2 cm; matrix size, 320 × 192; number of excitations (NEX), 1.00. The fat-saturation axial T2 images were obtained using the following parameters: TR/TE, 4000/75.8 ms; slice thickness, 7.0 mm with a gap of 1.0 mm; field of view, 38 cm × 38 cm; matrix size, 320 × 320; NEX, 2.00. The coronal T2 images were obtained using the following parameters: TR/TE, 2625/78.4 ms; slice thickness, 6.0 mm with a gap of 1.0 mm; field of view, 42 cm × 37.8 cm; matrix size, 352 × 288; NEX, 0.55. The total scanning time for each of the routine sequences was approximately 8 min. The IVIM was performed by using fat-suppressed, echo-planner imaging in the axial plane

with respiratory gating. The parallel imaging was used, and the parameters were as follows: TR/TE, 4286/61.2; slice thickness, 7.0 mm with a gap of 1.0 mm; field of view, 38 cm × 28.5 cm; matrix size, 128 × 128. Twelve *b* values ranging from 0 to 1200 s/mm^2 (10, 20, 40, 80, 100, 150, 200, 400, 600, 800, 1000, and 1200) were used, and the NEX for each *b* was 6, 4, 2, 2, 2, 1, 1, 2, 4, 6, 6, and 8. The total scanning time for the IVIM was approximately 10 min.

Image analysis

The data were quantitatively analyzed by using mono-exponential and bi-exponential models. The mono-exponential model that was used to estimate the ADC value was calculated from 12 *b* values and was described by the following equation: S(b)/S(0) = exp(-b × ADC) Where S(b) represents the signal intensity of diffusion sensitization at a given *b* value and S(0) represents the signal intensity of diffusion sensitization for *b* = 0 s/mm^2. IVIM-derived parameters with all *b*-value data on a pixel-by-pixel basis were calculated according to the following equation[15]: S(b)/S(0) = f exp(-b × D*) + (1-f)exp(-b × D) The bi-exponential IVIM model obtained pure diffusion coefficient (D), pseudo-diffusion coefficient (D*), and perfusion fraction (*f*) values. D was the diffusion coefficient that was representative of the pure molecular diffusivity, and D* was the perfusion parameter that was representative of the incoherent microcirculation (pseudodiffusion). The *f* value was the perfusion fraction that was linked to the microcirculation (pseudodiffusion).

All the images were obtained and transferred to a workstation (Advantage workstation 4.6; GE Medical System) and the data analysis was performed by two independent radiologists (Zhu S and Liu Y with 18 and 5 years of experience in reading MR images, respectively) who were blinded to the histopathological results. For each patient, as many of the MR images were selected for the measurement as possible from three consecutive slices of the DWI images, which covered the largest tumor portion, and the regions of interest (ROIs) were placed on the hepatic solid tumor components; the freehand ROI was placed to cover as much of the solid part of the tumor as possible. Exclusion of the areas of hemorrhage and necrosis was achieved by referring to the fat-saturation axial T2 images. The shape, size, and position of the ROIs were the same for each parameter map. The area of the ROIs ranged from 108 to 5202 mm^2 (the mean ROI area was 714 mm^2). The parametric values of the ROIs from the three imaging sections were averaged.

Pathologic examination

All the surgically resected specimens were subjected to hematoxylin and eosin staining of the tissue slices for the pathological evaluation. A pathologist (Sun T, with 21 years of experience reading histopathological slices) identified the pathological differentiation grades of each carcinoma, as well as the size and location of each, without knowing the MR findings. The pathological differentiation grade of each carcinoma was assessed according to the Edmondson and Steiner grading system[20].

Statistical analysis

The differences in the ADC and D among the different grades were analyzed using analysis of variance (ANOVA) and an LSD *t*-test, and the data are expressed as mean ± SD. The Kruskal-Wallis non-parametric test and paired comparisons were used to compare the D* and *f* values among the different grades. The quantitative data are presented as the median (interquartile range). The Spearman rank analysis was used to compare the correlation between the parameters and the histological grades. The correlation coefficient, rho (*r*), was obtained to compare the degree of the correlations as follows: little or no relationship if $r \geqslant 0$ but < 0.25; fair if $r \geqslant 0.25$ but < 0.5; moderate to good if $r \geq 0.5$ but < 0.75; and very good to excellent if $r \geqslant 0.75$. In addition, receiver operating characteristic (ROC) curve analyses were performed to evaluate the diagnostic performance of the parameters in distinguishing the low-grade (G1) and high-grade (G2 and G3) HCC. The areas under the ROC curves were obtained to compare the diagnostic capacities in terms of sensitivity, specificity, and accuracy, which were calculated with the optimal cutoff values being determined by the point of the largest Youden index for each parameter. The reproducibility of the ADCs and the IVIM-derived parameters of HCC was assessed by determination of the intra-class correlation coefficient (ICC), which reflected the differences in reliability between the two independent radiologists. ICC values less than 0.5 were indicative of poor reliability, values between 0.5 and 0.75 indicated moderate reliability, values between 0.75 and 0.9 indicated good reliability, and values greater than 0.90 indicated excellent reliability[21]. Bland-Altman analysis was used to evaluate the agreement between the inter-observer measurements. All statistical analyses were performed using SPSS19.0 software package (SPSS Inc, Chicago, IL, United States). A *P*-value less than 0.05 was considered to indicate statistical significance.

RESULTS

Comparison of the IVIM-DWI and conventional DWI parameters

Table 1 reports the ADC and IVIM parameters for the different histological grades of HCC. The ADC value, determined by both radiologists, of the G1 group was significantly higher than those of the G2 group and the G3 group ($P < 0.01$). For the IVIM parameters, the D value of the G3 group was significantly lower than those of the G2 group and the G1 group ($P < 0.01$). However, neither D* value nor the *f* value showed any statistical significance in distinguishing the three

Table 1 Intravoxel incoherent motion diffusion-weighted imaging parameters of different pathologic grades of hepatocellular carcinoma

Parameter	Observer	Edmondson-Steiner grade			*P* value
		1 (*n* = 14)	2 (*n* = 24)	3 (*n* = 24)	
ADC ($\times 10^{-3}$ mm^2/s)[1]	R1	1.496 ± 0.312	1.210 ± 0.186	1.003 ± 0.247	< 0.001
	R2	1.503 ± 0.306	1.214 ± 0.186	1.001 ± 0.236	< 0.001
D ($\times 10^{-3}$ mm^2/s)[1]	R1	1.186 ± 0.214	0.910 ± 0.151	0.775 ± 0.188	< 0.001
	R2	1.193 ± 0.226	0.910 ± 0.148	0.771 ± 0.187	< 0.001
D* ($\times 10^{-3}$ mm^2/s)[2]	R1	37.400 (43.900)	29.000 (71.700)	7.980 (63.590)	0.057
	R2	32.200 (44.600)	28.400 (74.363)	7.885 (61.640)	0.054
f (%)[2]	R1	27.250 (14.925)	20.675 (11.225)	31.300 (12.267)	0.149
	R2	26.550 (20.200)	21.200 (11.725)	31.550 (11.325)	0.214

[1]Data are mean ± SD, one-way analysis of variance; [2]data are median (interquartile range), Kruskal-Wallis Test. A *P*-value < 0.05 was considered statistically significant. R1: Radiologist 1; R2: Radiologist 2; ADC: Apparent diffusion coefficient; D: Pure diffusion coefficient; D*: Pseudo-diffusion coefficient; *f*: Perfusion fraction.

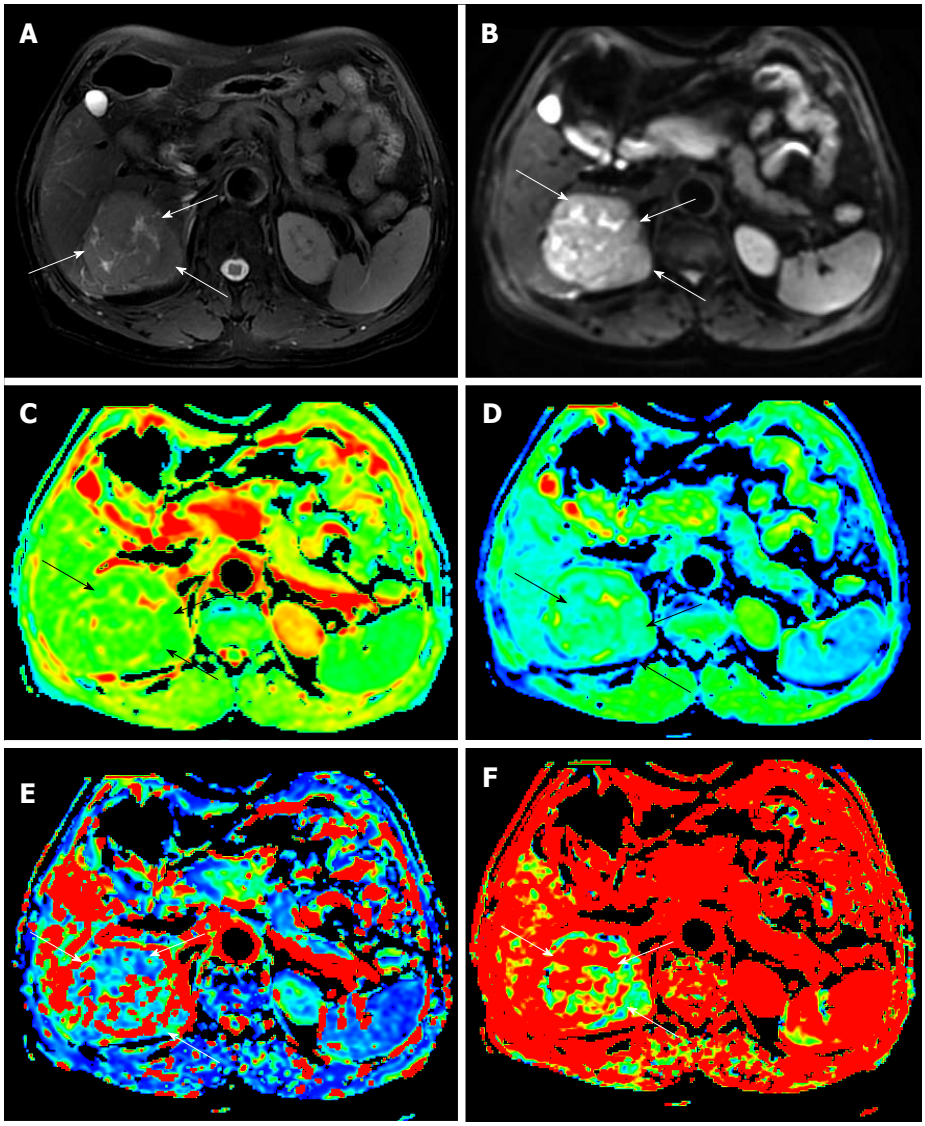

Figure 1 Magnetic resonance images of a 65-year-old man with an 8-cm surgically verified hepatocellular carcinoma with an Edmondson-Steiner grade 1. A: T2-weighted image; B: Diffusion-weighted image with a *b* value of 10 s/mm^2; C-F: Parametric maps (ADC, D, D*, and *f*, respectively) calculated from the IVIM diffusion-weighted imaging data. The tumor (white arrow) demonstrates a slightly high signal intensity on the T2-weighted image and a high signal intensity on the DWI image. The values of ADC, D, D*, and f for the ROIs of the HCC were 1.550 × 10^{-3} mm^2/s, 1.110 × 10^{-3} mm^2/s, 6.55 × 10^{-3} mm^2/s, and 0.387, respectively, which indicated an Edmondson-Steiner grade 1 HCC. HCC: Hepatocellular carcinoma; IVIM: Intravoxel incoherent motion; DWI: Diffusion-weighted imaging.

Table 2 Diagnostic value of intravoxel incoherent motion diffusion-weighted imaging and conventional diffusion-weighted imaging parameters in differentiating the low-grade group (G1) from the high-grade groups (G2 and G3)

Parameter	Observer	AUC (95%CI)	Optimal cutoff value	Youden index	Sensitivity (%)	Specificity (%)	Accuracy (%)
ADC	R1	0.843 (0.718, 0.968)	1.285	0.619	78.6(11/14)	83.3(40/48)	82.3(51/62)
	R2	0.852 (0.730, 0.974)	1.275	0.649	85.7(12/14)	79.2(38/48)	80.6(50/62)
D	R1	0.909 (0.834, 0.985)	0.962	0.741	92.9(13/14)	81.3(39/48)	83.9(52/62)
	R2	0.911 (0.832, 0.990)	0.977	0.804	92.9(13/14)	87.5(42/48)	88.7(55/62)
D*	R1	0.632 (0.489, 0.776)	17.75	0.378	85.7(12/14)	52.1(25/48)	59.7(37/62)
	R2	0.636 (0.495, 0.777)	17.90	0.378	85.7(12/14)	52.1(25/48)	59.7(37/62)
f	R1	0.523 (0.348, 0.698)	0.216	0.182	78.6(11/14)	39.6(19/48)	48.4(30/62)
	R2	0.518 (0.332, 0.704)	0.246	0.173	71.4(10/14)	45.8(22/48)	51.6(32/62)

R1: Radiologist 1; R2: Radiologist 2; ADC: Apparent diffusion coefficient; D: Pure diffusion coefficient; D*: Pseudo-diffusion coefficient; *f*: Perfusion fraction. ADC, D, and D* are in units of × 10^{-3} mm^2/s; f is in units of 100%; 95%CI: 95% confidence intervals.

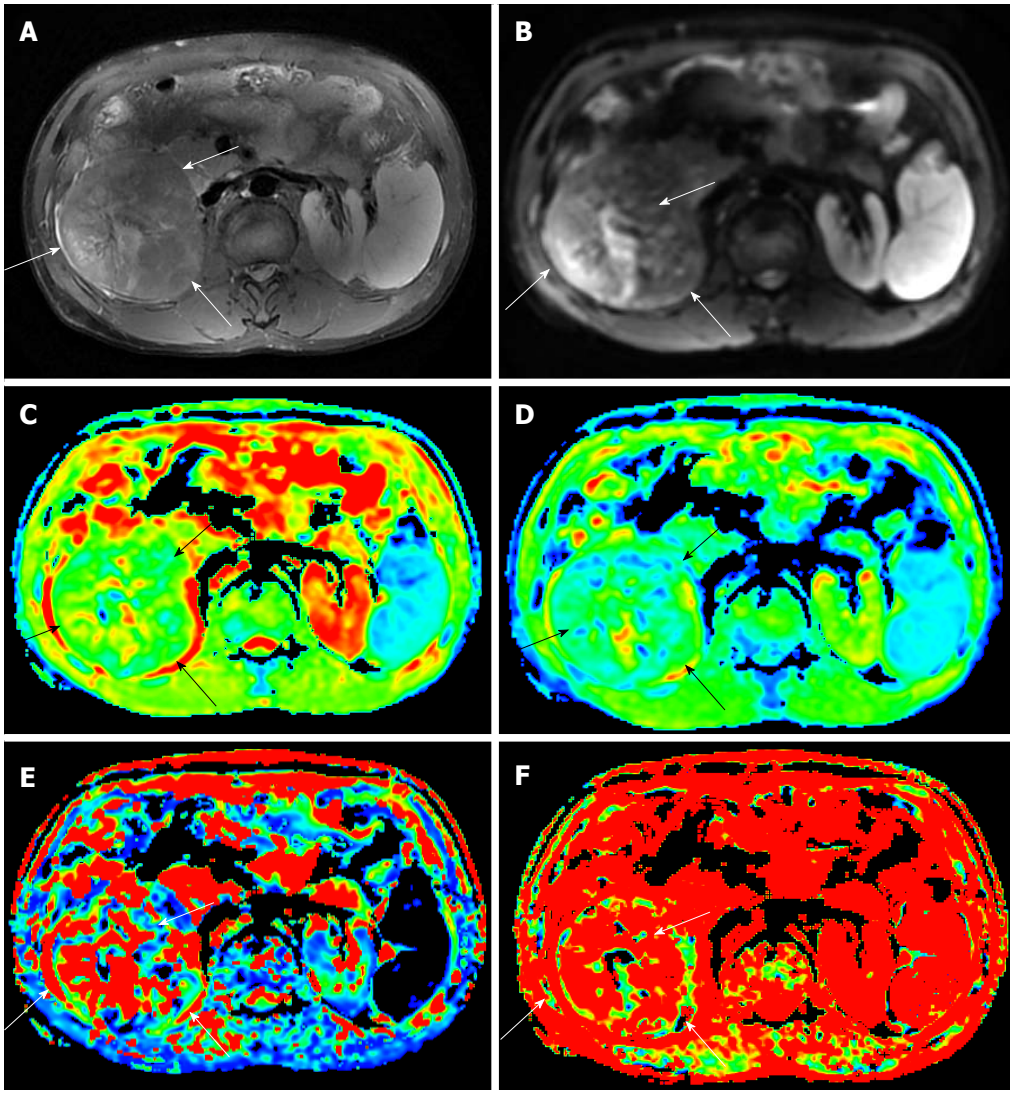

Figure 2 Magnetic resonance images of a 47-year-old man with a 10-cm surgically verified hepatocellular carcinoma of with an Edmondson-Steiner grade 2. A: T2-weighted image; B: Diffusion-weighted image with a *b* value of 10 s/mm^2; C-F: Parametric maps (ADC, D, D*, and *f*, respectively) calculated from the IVIM diffusion-weighted imaging data. The tumor (white arrow) demonstrates a slightly high signal intensity on the T2-weighted image and a high signal intensity on the DWI image. The values of the ADC, D, D*, and f for the ROIs of the HCC were 1.310 × 10^{-3} mm^2/s, 0.885 × 10^{-3} mm^2/s, 27.8 × 10^{-3} mm^2/s, and 0.450, respectively, which indicated an Edmondson-Steiner grade 2 HCC. HCC: Hepatocellular carcinoma; IVIM: Intravoxel incoherent motion; DWI: Diffusion-weighted imaging.

groups (P > 0.05). Figures 1-3 show representative grades 1-3 HCC, respectively. Figure 4 reports the quantitative comparison of the differences in the IVIM and DWI parameters among the three groups.

Table 3 Apparent diffusion coefficient and intravoxel incoherent motion derived parameters: Spearman correlation coefficients of the parameters with the histopathological grades

Spearman correlation			ADC	D	D*	*f*
R1	Grade	Correlation coefficient	-0.619	-0.628	-0.299	0.130
		P-value	< 0.001	< 0.001	0.018	0.313
R2	Grade	Correlation coefficient	-0.622	-0.633	-0.303	0.121
		P-value	< 0.001	< 0.001	0.017	0.349

P-value < 0.05 was considered statistically significant. ADC: Apparent diffusion coefficient; D: Pure diffusion coefficient; D*: Pseudo-diffusion coefficient; *f*: Perfusion fraction.

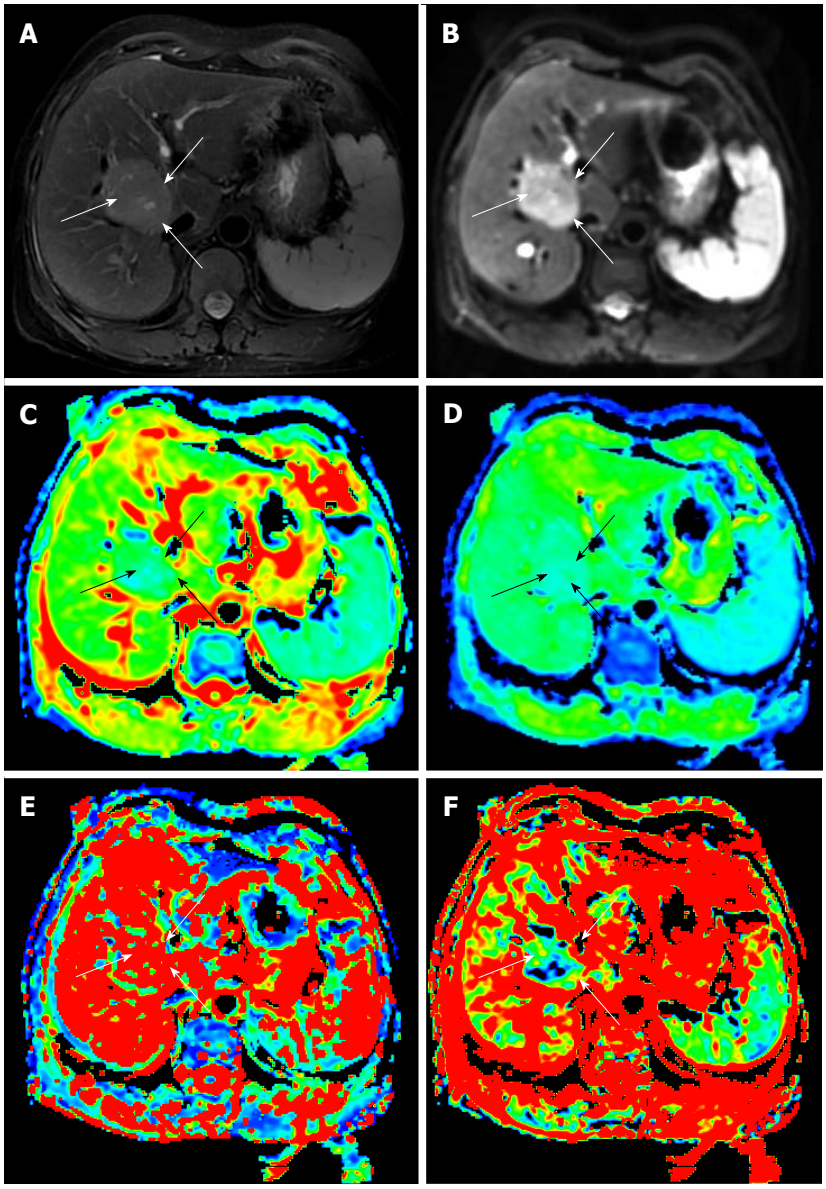

Figure 3 Magnetic resonance images of a 43-year-old woman with a 5-cm surgically verified hepatocellular carcinoma with an Edmondson-Steiner grade 3. A: T2-weighted image, B: Diffusion-weighted image with a *b* value of 10 s/mm^2; C-F: Parametric maps (ADC, D, D*, and *f*, respectively) calculated from the IVIM diffusion-weighted imaging data. The tumor (white arrow) demonstrates a slightly high signal intensity on the T2-weighted image and a high signal intensity on the DWI image. The values of the ADC, D, D*, and *f* for the ROIs of the HCC were 1.060 × 10^{-3} mm^2/s, 0.659 × 10^{-3} mm^2/s, 12.1 × 10^{-3} mm^2/s, and 0.109, respectively, which indicated an Edmondson-Steiner grade 3 HCC. HCC: Hepatocellular carcinomas; IVIM: Intravoxel incoherent motion; DWI: Diffusion-weighted imaging.

ROC analysis for diagnostic performance of the IVIM-DWI and conventional DWI parameters

The ROC curves obtained for differentiating the low-grade group (G1) from the high-grade groups (G2 and G3) are shown in Figure 5. The D showed the largest area under the curve (AUC) of 0.909 (95%CI: 0.834-0.985) obtained by radiologist 1 and 0.911 (95%CI: 0.832-0.990) obtained by radiologist 2. The

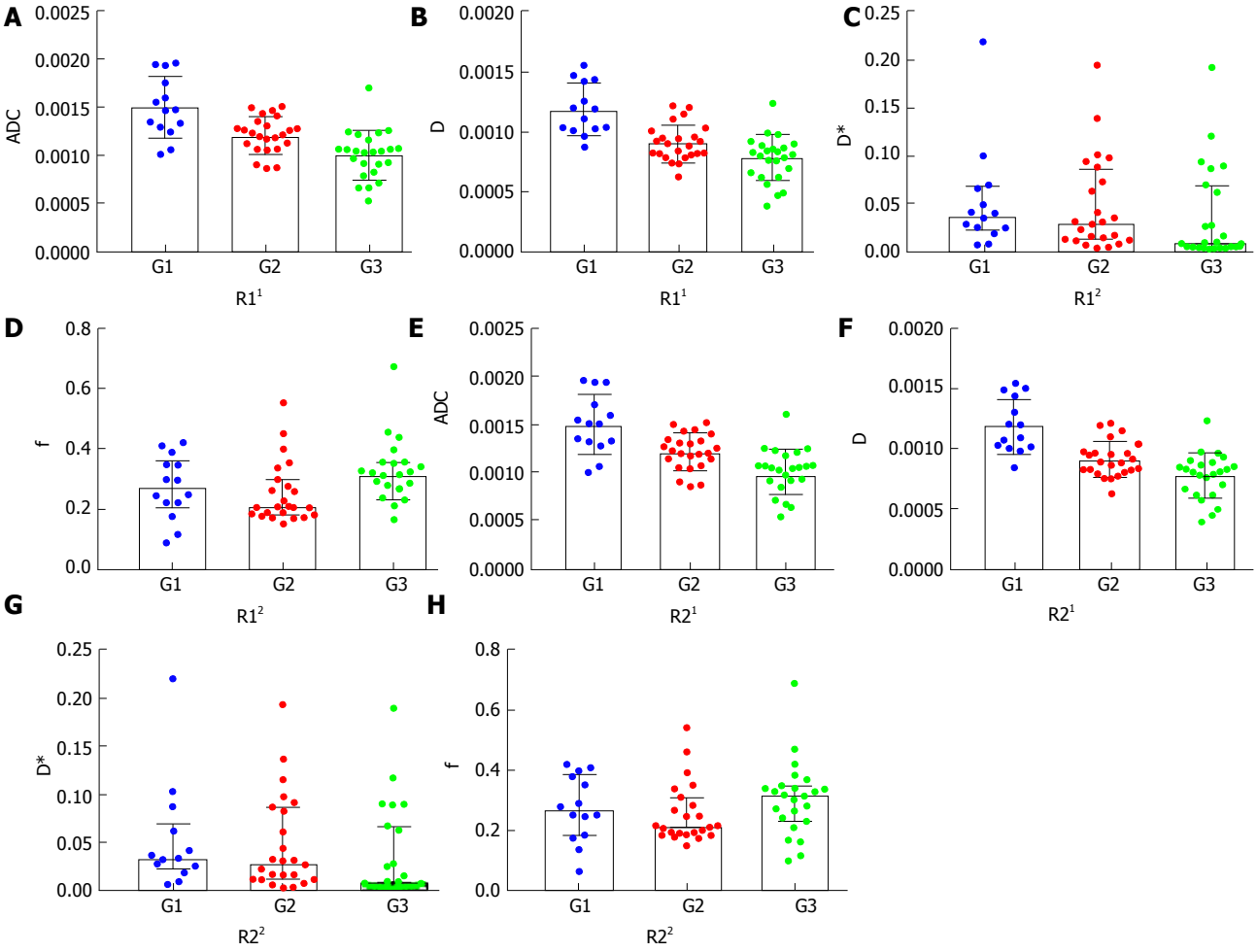

Figure 4 Column and scatter plot diagrams reporting the quantitative comparison of the differences in the intravoxel incoherent motion and conventional diffusion-weighted imaging parameters among the three groups of hepatocellular carcinoma. A-D: Quantitative comparison of the differences among the three groups in the ADC, D, D*, and f values, respectively, by radiologist 1; E and F: Quantitative comparison of the differences among the three groups in the ADC, D, D*, and f values, respectively, by radiologist 2. The differences in the ADC and D values among the different grades were statistically significant ($P < 0.001$); the differences between the G1 and G2, G1 and G3, and G2 and G3 were all statistically significant ($P < 0.05$). No statistical significance was found for the D* or the f values ($P > 0.05$). ADC, D, and D* are in units of mm2/s; f is in unit of 100%. 1Mean with SD; 2median with interquartile range. R1: Radiologist 1; R2: Radiologist 2; HCC: Hepatocellular carcinomas; IVIM: Intravoxel incoherent motion; DWI: Diffusion-weighted imaging, ADC: Apparent diffusion coefficient.

comparisons of the ROC curves of D, ADC, D*, and *f* values for discriminating the low-grade group from the high-grade groups demonstrated that the D and ADC values had similar diagnostic efficacy (AUC: 0.909 *vs* 0.843, respectively, $Z = 1.027$, $P = 0.3043$, measured by radiologist 1; 0.911 *vs* 0.852, respectively, $Z = 0.856$, $P = 0.3920$, measured by radiologist 2), while the D* and *f* values had lower diagnostic efficiency (AUC: 0.632 and 0.523, measured by radiologist 1; 0.636 and 0.518, measured by radiologist 2). No statistically significant differences were observed in the AUC values between the D* and the *f* ($Z = 0.734$, $P = 0.4631$, measured by radiologist 1; $Z = 1.625$, $P = 0.1041$, measured by radiologist 2) values. Table 2 shows the sensitivity, specificity, and accuracy of the IVIM-DWI and conventional DWI parameters at the optimal cutoff values of differentiating the low-grade group from the high-grade groups.

Correlation of IVIM-DWI and conventional DWI parameters with the histopathological results

Table 3 reports the correlation coefficients between the parameters and the histopathological grades. For radiologist 1, the Spearman correlation analysis demonstrated that there was a moderate to good relationship between the pathologically differentiated grade and the ADC ($r = -0.619$, $P < 0.001$), as well as the D ($r = -0.628$, $P < 0.001$) and D*, which demonstrated a fair relationship with the pathologically differentiated grade ($r = -0.299$, $P = 0.018$), but no statistical significance was obtained regarding the correlation between the pathologic grade and the *f* value ($r = 0.130$, $P = 0.313$). Moreover, the correlation coefficients for the ADC ($r = -0.622$, $P < 0.001$), D ($r = -0.633$, $P < 0.001$) and D* ($r = -0.303$, $P = 0.017$) that were obtained by radiologist 2 were also correlated with the pathologically differentiated grade, and the *f* value (*r*

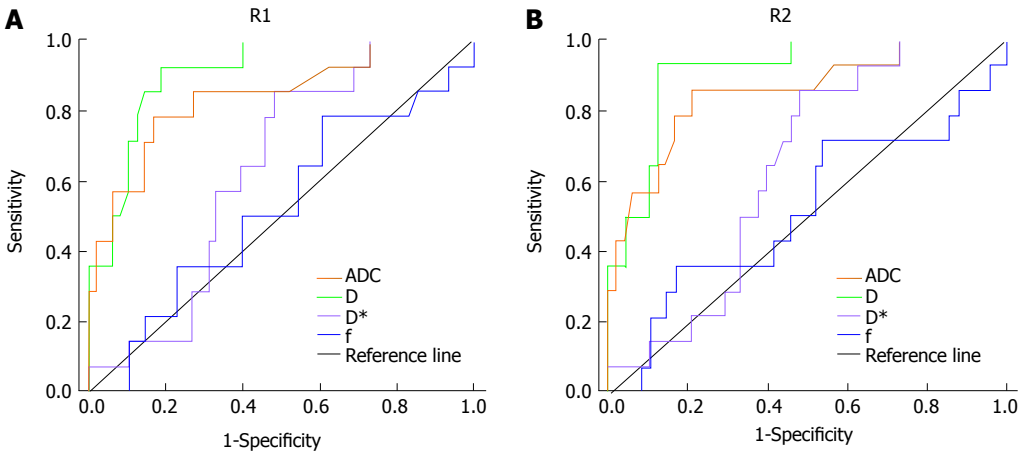

Figure 5 Graphs showing that receiver operating characteristic curves of the intravoxel incoherent motion- diffusion-weighted imaging and conventional diffusion-weighted imaging parameters of hepatocellular carcinoma for differentiating the low-grade group from the high-grade groups, as measured by the two radiologists. A: ROC curves of the parameters of HCC by radiologist 1; B: ROC curves of the parameters of HCC by radiologist 2. The area under curve (AUC) for D was the largest of all the parameters obtained by the two radiologists. R1: Radiologist 1; R2: Radiologist 2; HCC: Hepatocellular carcinomas; IVIM: Intravoxel incoherent motion; DWI: Diffusion-weighted imaging, ADC: Apparent diffusion coefficient; D: Pure diffusion coefficient; D*: Pseudo-diffusion coefficient; *f*: Perfusion fraction.

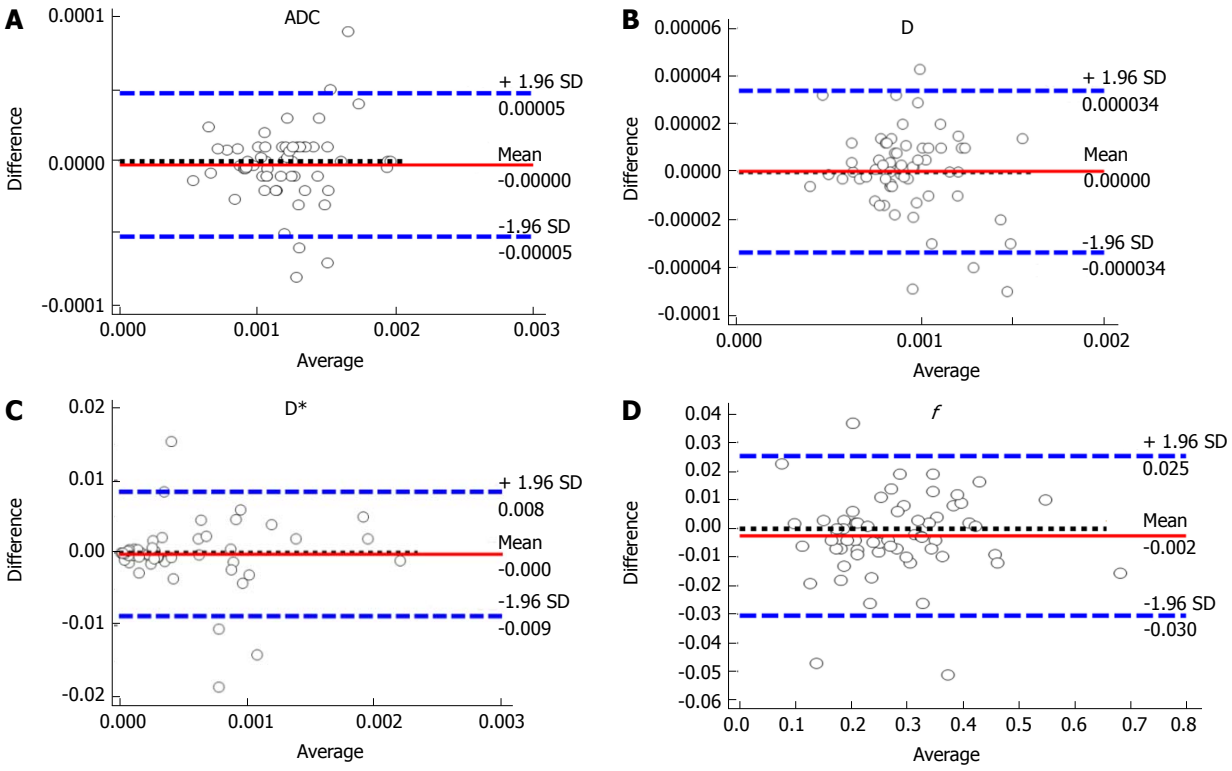

Figure 6 Bland-Altman plots showing the distribution of the differences of the intravoxel incoherent motion diffusion-weighted imaging and conventional diffusion-weighted imaging parameters between the two radiologists. A-D: The distribution of the differences of the ADC, D, D*, and f values, respectively. The differences between measurements by the two radiologists regarding the parameters were relatively small. ±1.95 SD indicates 95% limits of agreement, mean, and mean difference, ADC: Apparent diffusion coefficient.

= 0.121, *P* = 0.349) showed no statistical significance.

Inter-observer reproducibility

The ICCs between the two observers were 0.996 (95%CI: 0.994-0.998) for ADC, 0.997 (95%CI: 0.996-0.998) for D, 0.996 (95%CI: 0.996-0.998) for D*, and 0.992 (95%CI: 0.987-0.995) for the *f* value. The results suggested that there was an excellent agreement between the two observers for all the parameters. Figure 6 shows the reliability of the inter-observer measurements in the IVIM and ADC parameters, as assessed by the Bland-Altman analysis.

DISCUSSION

IVIM-based DWI is a functional and non-contrast-

enhanced MR imaging technique that can obtain diffusion and perfusion information simultaneously. IVIM-DWI has become an evaluation model of tumor microenvironment, showing changes in the microstructure of tissues and of microcirculation. IVIM-DWI may allow cancer to be evaluated more precisely, and it has been used as a diagnostic tool for several organs, including the pancreas, kidney, brain, breast, and liver[22-27]. Recent studies have indicated that accurate differentiation of HCC with different pathological grades is an important issue that should be considered in the planning of treatment strategies and prognostic evaluations[28,29]. Thus, an effective method is needed to evaluate the tumor cell differentiation grade and predict the prognosis.

In this study, both the ADC and D values showed statistically significant differences among the different grades. As the pathological grade increased, the numeric value gradually decreased; the values of the G3 group were lower than those of the G2 and G1 groups. Water mobility is restricted in malignant tissue due to an increase in the cellular density and a decrease in the interstitial space. These results regarding HCC may be attributable to the increased cellular density, nuclear-to-cytoplasmic ratios, and architectural complications when comparing the G3 and G2 groups to the G1 group, which resulted in the decreased ADC and D values[30]. Sungmin Woo *et al*[16] demonstrated that ADC and D values are both significantly lower in high-grade HCC than in low-grade HCC, which is consistent with the current findings. Previous studies in tumors elsewhere in the body also showed similar results[31,32]. The other IVIM-derived parameters, including the D* and *f* values, were not statistically significant in differentiating the G1, G2, and G3 groups. The D* and *f* values are the perfusion parameters, which could be used to reflect the vascularity of the tissue. According to the IVIM theory, D* is defined as the average blood velocity and the mean capillary segment length, and *f* measures the fractional blood volume of the microcirculation[15]. Therefore, the results of the D* and *f* values may be related to the location of the lesion and the feeding artery. Furthermore, previous studies have reported that the D* and *f* values are not accurate in the assessment of the tumor differentiation grades because of their intrinsic instability, poor reproducibility, and lower diagnostic efficiency[33,34]. Nevertheless, Vincenza Granata *et al*[18] demonstrated that the *f* values were significantly different in the HCC groups with G1, G2, and G3 histological grades, and a significant correlation was reported between the *f* value and the histologic grade, which is in disagreement with our results. Thus, the relationship between perfusion parameters and the histological grade remains controversial.

In the present study, the IVIM-derived D and ADC values showed significantly better diagnostic performance than the D* and f values in differentiating low-grade from high-grade HCC, according to the ROC analysis. The AUC values for the D and ADC in differentiating the histologic grades of HCC were not significantly different (AUC: 0.909 *vs* 0.843, respectively, $Z = 1.027$, $P = 0.3043$, by radiologist 1; 0.911 *vs* 0.852, respectively, $Z = 0.856$, $P = 0.3920$, by radiologist 2). Because the higher the *b*-value is, the more sensitive the sequence is to diffusion effects[9], the perfusion effect could be avoided if the mono-exponential fit was performed using high *b* values (> 200 s/mm^2); perfusion may have a small contribution to the ADC value, which leads to the similar results found in the D and ADC values[25]. And, the results were comparable to the values reported in the literature[25]. However, in our study, the D value showed greater AUC, sensitivity, and accuracy than the ADC value. In addition, both the D and ADC values were significantly correlated with the histological grade of HCC, as well as with the D ($r = -0.628$, $P < 0.001$, measured by radiologist 1; $r = -0.633$, $P < 0.001$, measured by radiologist 2) and ADC ($r = -0.619$, $P < 0.001$, measured by radiologist 1; $r = -0.622$, $P < 0.001$, measured by radiologist 2) values, which demonstrated a moderate to good correlation between D and the histological grade, and between ADC and the histological grade.

Our study had several limitations. First, this study was retrospective; thus, there may have been potential bias in the patient selection. Second, the study population was relatively small, and there were no cases of Edmondson-Steiner grade 4. Therefore, further studies with more samples are still needed. Third, the ROIs were mainly selected on the solid parts of the carcinoma; meanwhile, we did not obtain histopathologic verification of the whole tumor. Therefore, we could not examine the exact histological grade of the "solid" region where an ROI was placed, which may have led to selection discordance. Fourth, some of the ROIs were set in the left liver lobe, which is prone to be influenced by adjacent organ functions, such as heart and diaphragm motion or gastrointestinal peristalsis. Finally, further studies to validate the IVIM perfusion parameters are essential to be correlated with the DCE-MRI parameters and reflect the perfusion characteristics of a tumor.

In conclusion, D and ADC values showed better diagnostic performance in differentiating high-grade HCC from low-grade HCC than D* and *f* values, and a moderate to good correlation was observed between the ADC and D values and the histological grades.

ARTICLE HIGHLIGHTS

Research background

Hepatocellular carcinoma (HCC) is the most common primary malignant tumor of the liver. It is the fifth most important cancer worldwide and the third leading cause of cancer-related death. The pathological grade of HCC is heavily associated with the prognosis. However, it is difficult to provide a prediction of accurate preoperative pathological grade of HCC using routine imaging modalities.

Diffusion-weighted imaging (DWI) is a noninvasive approach to sensitively evaluate the small-scale motion of water molecules at the microscopic level. However, it is limited in that the ADC fails to evaluate the water molecular diffusion in tissues precisely. The IVIM approach uses a bi-exponential function to describe the DWI data and it is possible to obtain additional quantitative parameters that describe water diffusivity, perfusion (pseudodiffusion

coefficient), and the perfusion fraction of tissues. Recently, IVIM-DWI has been used to investigate the correlation between the parameters involved in the histologic grade of HCC. This study can determine a new imaging technique to assess the histological grade of HCC and predict the patient's prognosis in clinical practice.

Research motivation

This study investigated the value of the IVIM-derived parameters and conventional DWI-derived parameters for predicting the histological grade of HCC, evaluated the diagnostic efficiency of the parameters in distinguishing the pathological grades of HCC, and assessed the correlation between the parameters and the histological grades. With the help of the parameters, we can determine the pathological grade of HCC without the pathological results of surgery. The pathological grade of HCC is heavily associated with the prognosis. Therefore, we can assess the pathological grade of HCC and predict the patient prognosis, simultaneously.

Research objectives

The present study was to compare IVIM-derived parameters with conventional DWI-derived ADC values for determining the histologic grades of HCC and evaluated the correlation between the parameters and the histological grades. The parameters derived from IVIM-DWI and conventional DWI showed statistical significance in different histologic grades of HCC, and they will have diagnostic value in differentiating the pathological grades, as the correlation was observed between the parameters and grades. The results showed that these parameters are of great significance in the diagnosis of the pathological grades of HCC. DWI-MR will be a new imaging technique to assess the pathological grade of an HCC, which might be helpful in predicting the patient prognosis.

Research methods

A retrospective study was performed. Sixty-two patients (50 men and 12 women; mean age, 54.31 ± 9.36 years; range, 30-76 years) with surgically confirmed HCC underwent diffusion-weighted magnetic resonance imaging with twelve *b* values (10-1200 s/mm^2). All the tumors were histologically classified according to the major Edmondson-Steiner grade on the final pathologic reports as follows: grade 1 (n = 14), grade 2 (n = 24), grade 3 (n = 24), and grade 4 (n = 0). The apparent diffusion coefficient (ADC), pseudo-diffusion coefficient (D*), pure diffusion coefficient (D), and perfusion fraction (f) were calculated by two radiologists. The IVIM and conventional DWI parameters were compared among different grades by using analysis of variance (ANOVA) and the Kruskal-Wallis test. Receiver operating characteristic (ROC) analysis was performed to evaluate the diagnostic efficiency of distinguishing between low-grade (G1) and high-grade (G2 and G3) HCC. The correlations between the parameters and the histological grades were assessed by using the Spearman correlation test. Bland-Altman analysis was used to evaluate the reproducibility of the two radiologists' measurements. The measurement reproducibility between the two observers shows the reliability of parameters, and it makes sure that the results for the study objectives are more persuasive, which is the characteristics and novelty.

Research results

The differences in the ADC and D values among the groups with G1, G2, and G3 histological grades of HCC were statistically significant (P < 0.001). The D* and f values had no significant differences among the different histological grades of HCC (P > 0.05). The ROC analyses demonstrated that the D and ADC values had better diagnostic performance in differentiating the low-grade HCC from the high-grade HCC, with areas under the curve (AUCs) of 0.909 and 0.843, respectively, measured by radiologist 1 and of 0.911 and 0.852, respectively, measured by radiologist 2. The following significant correlations were obtained between the ADC, D, and D* values and the histological grades: r = -0.619 (P < 0.001), r = -0.628 (P < 0.001), and r = -0.299 (P = 0.018), respectively, as measured by radiologist 1; r = -0.622 (P < 0.001), r = -0.633 (P < 0.001), and r = -0.303 (P = 0.017), respectively, as measured by radiologist 2. The intra-class correlation coefficient (ICC) values between the two observers were 0.996 for ADC, 0.997 for D, 0.996 for D*, and 0.992 for the f values, which indicated excellent inter-observer agreement in the measurements between the two observers.

The problem that remains to be solved is that the significance of the perfusion parameters (D* and f) among different histological grades of HCC and the correlation between perfusion parameters and the histological grade are in disagreement with previous results, which remains controversial. At the same time, further studies should investigate the cor relation between the IVIM perfusion parameters and the DCE-MRI parameters to reflect the perfusion characteristics of tumor.

Research conclusions

DWI-MR imaging can be used as a noninvasive quantitative imaging method in discriminating different histological grades of HCC. DWI-MR is a noninvasive approach to sensitively evaluate the small-scale motion of water molecules at the microscopic level, reflect tumor microenvironment, show changes in the microcirculation of tissues, and provide the pathology and physiology information. IVIM-DWI parameters and conventional DWI parameters might be useful in assessing the differentiation grades of carcinoma, which might be helpful in predicting the patient prognosis. The study showed that the perfusion parameters (D* and f) were not statistically significant in differentiating the histological grades of HCC, and showed significant lower diagnostic performance in differentiating low-grade (G1) from high-grade (G2 and G3) HCCs. These results may be related to the location of the lesion and the feeding artery. IVIM-derived parameters and conventional DWI parameters can predict the histological grade of HCC and the correlation was observed between the parameters and the histological grades. The measurement reproducibility of the parameters was excellent between the two radiologists. The measured values of the D* and f existed instability in all patients, and the diagnostic value of the D*and f remains controversial. The IVIM-derived D and ADC values showed better diagnostic performance in differentiating high-grade HCC from low-grade HCC, and a moderate to good correlation was observed between the ADC and D values and the histological grades. IVIM-DWI parameters and conventional DWI parameter might be useful in evaluating the differentiation grades of carcinomas before operation, which might be helpful in predicting the patient prognosis in clinical practice.

Research perspectives

In the MR examination, the total scanning time for the IVIM was related to the respiratory condition of the patient. The faster the breathing, the shorter the scanning time. The total scanning time of all the patients is approximately 8-13 min, and the average time is about 10 min. In the process of the measurement, it should be repeated to ensure the stability and reliability of the parameters. Further studies to validate the IVIM perfusion parameters are essential to be correlated with the DCE-MRI parameters and reflect the perfusion characteristics of tumor. At the same time, the texture information of tumors can be analyzed, which can reflect the essential characteristics of the mass. Radiomics is a new research method for tumors. According to the heterogeneity of tumors, a large number of high dimensional quantitative image features are extracted from MRI, PET, and CT images and analyzed. By extracting and analyzing the characteristics of medical images, it can evaluate the diagnosis and prognosis of patients.

REFERENCES

1 **Kew MC**. Epidemiology of hepatocellular carcinoma. *Toxicology* 2002; **181-182**: 35-38 [PMID: 12505281 DOI: 10.1016/S0300-483X(02)00251-2]

2 **Gomaa AI**, Khan SA, Toledano MB, Waked I, Taylor-Robinson SD. Hepatocellular carcinoma: epidemiology, risk factors and pathogenesis. *World J Gastroenterol* 2008; **14**: 4300-4308 [PMID: 18666317 DOI: 10.3748/wjg.14.4300]

3 **Parkin DM**. Global cancer statistics in the year 2000. *Lancet Oncol* 2001; **2**: 533-543 [PMID: 11905707 DOI: 10.1016/S1470-2045(01)00486-7]

4 **Parkin DM**, Bray F, Ferlay J, Pisani P. Global cancer statistics, 2002. *CA Cancer J Clin* 2005; **55**: 74-108 [PMID: 15761078 DOI: 10.3322/canjclin.55.2.74]

5 **Zhou L**, Rui JA, Wang SB, Chen SG, Qu Q, Chi TY, Wei X, Han K, Zhang N, Zhao HT. Factors predictive for long-term survival of male patients with hepatocellular carcinoma after curative resection. *J Surg Oncol* 2007; **95**: 298-303 [PMID: 17326130 DOI: 10.1002/jso.20678]

6 **Zhou L**, Rui JA, Ye DX, Wang SB, Chen SG, Qu Q. Edmondson-Steiner grading increases the predictive efficiency of TNM staging for long-term survival of patients with hepatocellular carcinoma

after curative resection. *World J Surg* 2008; **32**: 1748-1756 [PMID: 18493820 DOI: 10.1007/s00268-008-9615-8]
7 **Stigliano R**, Marelli L, Yu D, Davies N, Patch D, Burroughs AK. Seeding following percutaneous diagnostic and therapeutic approaches for hepatocellular carcinoma. What is the risk and the outcome? Seeding risk for percutaneous approach of HCC. *Cancer Treat Rev* 2007; **33**: 437-447 [PMID: 17512669 DOI: 10.1016/j.ctrv.2007.04.001]
8 **Bruix J**, Sherman M; Practice Guidelines Committee, American Association for the Study of Liver Diseases. Management of hepatocellular carcinoma. *Hepatology* 2005; **42**: 1208-1236 [PMID: 16250051 DOI: 10.1002/hep.20933]
9 **Kele PG**, van der Jagt EJ. Diffusion weighted imaging in the liver. *World J Gastroenterol* 2010; **16**: 1567-1576 [PMID: 20355235 DOI: 10.3748/wjg.v16.i13.1567]
10 **Baliyan V**, Das CJ, Sharma R, Gupta AK. Diffusion weighted imaging: Technique and applications. *World J Radiol* 2016; **8**: 785-798 [PMID: 27721941 DOI: 10.4329/wjr.v8.i9.785]
11 **Iima M**, Le Bihan D. Clinical Intravoxel Incoherent Motion and Diffusion MR Imaging: Past, Present, and Future. *Radiology* 2016; **278**: 13-32 [PMID: 26690990 DOI: 10.1148/radiol.2015150244]
12 **Koh DM**, Collins DJ, Orton MR. Intravoxel incoherent motion in body diffusion-weighted MRI: reality and challenges. *AJR Am J Roentgenol* 2011; **196**: 1351-1361 [PMID: 21606299 DOI: 10.2214/AJR.10.5515]
13 **Filli L**, Wurnig MC, Luechinger R, Eberhardt C, Guggenberger R, Boss A. Whole-body intravoxel incoherent motion imaging. *Eur Radiol* 2015; **25**: 2049-2058 [PMID: 25576232 DOI: 10.1007/s00330-014-3577-z]
14 **Le Bihan D**, Breton E, Lallemand D, Grenier P, Cabanis E, Laval-Jeantet M. MR imaging of intravoxel incoherent motions: application to diffusion and perfusion in neurologic disorders. *Radiology* 1986; **161**: 401-407 [PMID: 3763909 DOI: 10.1148/radiology.161.2.3763909]
15 **Le Bihan D**, Breton E, Lallemand D, Aubin ML, Vignaud J, Laval-Jeantet M. Separation of diffusion and perfusion in intravoxel incoherent motion MR imaging. *Radiology* 1988; **168**: 497-505 [PMID: 3393671 DOI: 10.1148/radiology.168.2.3393671]
16 **Woo S**, Lee JM, Yoon JH, Joo I, Han JK, Choi BI. Intravoxel incoherent motion diffusion-weighted MR imaging of hepatocellular carcinoma: correlation with enhancement degree and histologic grade. *Radiology* 2014; **270**: 758-767 [PMID: 24475811 DOI: 10.1148/radiol.13130444]
17 **Nakanishi M**, Chuma M, Hige S, Omatsu T, Yokoo H, Nakanishi K, Kamiyama T, Kubota K, Haga H, Matsuno Y, Onodera Y, Kato M, Asaka M. Relationship between diffusion-weighted magnetic resonance imaging and histological tumor grading of hepatocellular carcinoma. *Ann Surg Oncol* 2012; **19**: 1302-1309 [PMID: 21927976 DOI: 10.1245/s10434-011-2066-8]
18 **Granata V**, Fusco R, Catalano O, Guarino B, Granata F, Tatangelo F, Avallone A, Piccirillo M, Palaia R, Izzo F, Petrillo A. Intravoxel incoherent motion (IVIM) in diffusion-weighted imaging (DWI) for Hepatocellular carcinoma: correlation with histologic grade. *Oncotarget* 2016; **7**: 79357-79364 [PMID: 27764817 DOI: 10.18632/oncotarget.12689]
19 **Andreou A**, Koh DM, Collins DJ, Blackledge M, Wallace T, Leach MO, Orton MR. Measurement reproducibility of perfusion fraction and pseudodiffusion coefficient derived by intravoxel incoherent motion diffusion-weighted MR imaging in normal liver and metastases. *Eur Radiol* 2013; **23**: 428-434 [PMID: 23052642 DOI: 10.1007/s00330-012-2604-1]
20 **Edmondson HA**, Steiner PE. Primary carcinoma of the liver: a study of 100 cases among 48,900 necropsies. *Cancer* 1954; **7**: 462-503 [PMID: 13160935]
21 **Koo TK**, Li MY. A Guideline of Selecting and Reporting Intraclass Correlation Coefficients for Reliability Research. *J Chiropr Med* 2016; **15**: 155-163 [PMID: 27330520 DOI: 10.1016/j.jcm.2016.02.012]
22 **Fujima N**, Yoshida D, Sakashita T, Homma A, Tsukahara A, Tha KK, Kudo K, Shirato H. Intravoxel incoherent motion diffusion-weighted imaging in head and neck squamous cell carcinoma: assessment of perfusion-related parameters compared to dynamic contrast-enhanced MRI. *Magn Reson Imaging* 2014; **32**: 1206-1213 [PMID: 25131628 DOI: 10.1016/j.mri.2014.08.009]
23 **Chandarana H**, Lee VS, Hecht E, Taouli B, Sigmund EE. Comparison of biexponential and monoexponential model of diffusion weighted imaging in evaluation of renal lesions: preliminary experience. *Invest Radiol* 2011; **46**: 285-291 [PMID: 21102345 DOI: 10.1097/RLI.0b013e3181ffc485]
24 **Concia M**, Sprinkart AM, Penner AH, Brossart P, Gieseke J, Schild HH, Willinek WA, Mürtz P. Diffusion-weighted magnetic resonance imaging of the pancreas: diagnostic benefit from an intravoxel incoherent motion model-based 3 b-value analysis. *Invest Radiol* 2014; **49**: 93-100 [PMID: 24089021 DOI: 10.1097/RLI.0b013e3182a71cc3]
25 **Liu C**, Liang C, Liu Z, Zhang S, Huang B. Intravoxel incoherent motion (IVIM) in evaluation of breast lesions: comparison with conventional DWI. *Eur J Radiol* 2013; **82**: e782-e789 [PMID: 24034833 DOI: 10.1016/j.ejrad.2013.08.006]
26 **Guo W**, Zhao S, Yang Y, Shao G. Histological grade of hepatocellular carcinoma predicted by quantitative diffusion-weighted imaging. *Int J Clin Exp Med* 2015; **8**: 4164-4169 [PMID: 26064326]
27 **Nishie A**, Tajima T, Asayama Y, Ishigami K, Kakihara D, Nakayama T, Takayama Y, Okamoto D, Fujita N, Taketomi A, Yoshimitsu K, Honda H. Diagnostic performance of apparent diffusion coefficient for predicting histological grade of hepatocellular carcinoma. *Eur J Radiol* 2011; **80**: e29-e33 [PMID: 20619566 DOI: 10.1016/j.ejrad.2010.06.019]
28 **Kim SH**, Lim HK, Choi D, Lee WJ, Kim SH, Kim MJ, Kim CK, Jeon YH, Lee JM, Rhim H. Percutaneous radiofrequency ablation of hepatocellular carcinoma: effect of histologic grade on therapeutic results. *AJR Am J Roentgenol* 2006; **186**: S327-S333 [PMID: 16632696 DOI: 10.2214/AJR.05.0350]
29 **Jonas S**, Bechstein WO, Steinmüller T, Herrmann M, Radke C, Berg T, Settmacher U, Neuhaus P. Vascular invasion and histopathologic grading determine outcome after liver transplantation for hepatocellular carcinoma in cirrhosis. *Hepatology* 2001; **33**: 1080-1086 [PMID: 11343235 DOI: 10.1053/jhep.2001.23561]
30 **Muhi A**, Ichikawa T, Motosugi U, Sano K, Matsuda M, Kitamura T, Nakazawa T, Araki T. High-b-value diffusion-weighted MR imaging of hepatocellular lesions: estimation of grade of malignancy of hepatocellular carcinoma. *J Magn Reson Imaging* 2009; **30**: 1005-1011 [PMID: 19856432 DOI: 10.1002/jmri.21931]
31 **Togao O**, Hiwatashi A, Yamashita K, Kikuchi K, Mizoguchi M, Yoshimoto K, Suzuki SO, Iwaki T, Obara M, Van Cauteren M, Honda H. Differentiation of high-grade and low-grade diffuse gliomas by intravoxel incoherent motion MR imaging. *Neuro Oncol* 2016; **18**: 132-141 [PMID: 26243792 DOI: 10.1093/neuonc/nov147]
32 **Yang DM**, Kim HC, Kim SW, Jahng GH, Won KY, Lim SJ, Oh JH. Prostate cancer: correlation of intravoxel incoherent motion MR parameters with Gleason score. *Clin Imaging* 2016; **40**: 445-450 [PMID: 27133684 DOI: 10.1016/j.clinimag.2016.01.001]
33 **Sun H**, Xu Y, Xu Q, Shi K, Wang W. Rectal cancer: Short-term reproducibility of intravoxel incoherent motion parameters in 3.0T magnetic resonance imaging. *Medicine* (Baltimore) 2017; **96**: e6866 [PMID: 28489784 DOI: 10.1097/MD.0000000000006866]
34 **Luo M**, Zhang L, Jiang XH, Zhang WD. Intravoxel Incoherent Motion Diffusion-weighted Imaging: Evaluation of the Differentiation of Solid Hepatic Lesions. *Transl Oncol* 2017; **10**: 831-838 [PMID: 28866259 DOI: 10.1016/j.tranon.2017.08.003]

P- Reviewer: Mendez-Sanchez N **S- Editor**: Ma YJ
L- Editor: Wang TQ **E- Editor**: Ma YJ

Published by **Baishideng Publishing Group Inc**
7901 Stoneridge Drive, Suite 501, Pleasanton, CA 94588, USA
Telephone: +1-925-223-8242
Fax: +1-925-223-8243
E-mail: bpgoffice@wjgnet.com
Help Desk: http://www.f6publishing.com/helpdesk
http://www.wjgnet.com

ISSN 1007-9327

© 2018 Baishideng Publishing Group Inc. All rights reserved.